Neutrino Detectors

Sina Bahrasemani

November 15, 2017

Outline

Neutrino

Neutrino is so named because it is electrically neutral and because its rest mass is so small (-ino) that it was originally thought to be zero.

Neutrino

Neutrino is so named because it is electrically neutral and because its rest mass is so small (-ino) that it was originally thought to be zero.

- neutrino was postulated first by Wolfgang Pauli in 1930 to explain how beta decay could conserve energy, momentum, and angular momentum (spin).

Neutrino

Neutrino is so named because it is electrically neutral and because its rest mass is so small (-ino) that it was originally thought to be zero.

- neutrino was postulated first by Wolfgang Pauli in 1930 to explain how beta decay could conserve energy, momentum, and angular momentum (spin).
- neutrinos typically pass through normal matter unimpeded and undetected.

Neutrino

Neutrino is so named because it is electrically neutral and because its rest mass is so small (-ino) that it was originally thought to be zero.

- neutrino was postulated first by Wolfgang Pauli in 1930 to explain how beta decay could conserve energy, momentum, and angular momentum (spin).
- neutrinos typically pass through normal matter unimpeded and undetected.
- The assumption that neutrinos are massless and characterised by distinct, individual lepton numbers was incorporated into the theory of electro-weak interactions.

Neutrino mysteries

- **Generations:** neutrinos come in three leptonic flavors

$$\begin{pmatrix} e \\ \nu_e \end{pmatrix} \quad \begin{pmatrix} \mu \\ \nu_\mu \end{pmatrix} \quad \begin{pmatrix} \tau \\ \nu_\tau \end{pmatrix}$$

Neutrino mysteries

- **Generations:** neutrinos come in three leptonic flavors

$$\begin{pmatrix} e \\ \nu_e \end{pmatrix} \quad \begin{pmatrix} \mu \\ \nu_\mu \end{pmatrix} \quad \begin{pmatrix} \tau \\ \nu_\tau \end{pmatrix}$$

- **Oscillation:** nueutrinos travel through space as waves that have a different frequency. The flavor of a neutrino is determined as a superposition of the mass eigenstates. The type of the flavor oscillates, because the phase of the wave changes.

- **Generations:** neutrinos come in three leptonic flavors

$$\begin{pmatrix} e \\ \nu_e \end{pmatrix} \quad \begin{pmatrix} \mu \\ \nu_\mu \end{pmatrix} \quad \begin{pmatrix} \tau \\ \nu_\tau \end{pmatrix}$$

- **Oscillation:** nueutrinos travel through space as waves that have a different frequency. The flavor of a neutrino is determined as a superposition of the mass eigenstates. The type of the flavor oscillates, because the phase of the wave changes.
- **Mass:** there are three discrete neutrino masses with different tiny values, but they do not correspond uniquely to the three flavors ($m_{\nu_l} < 10^{-7} m_e$)

Reactor neutrinos

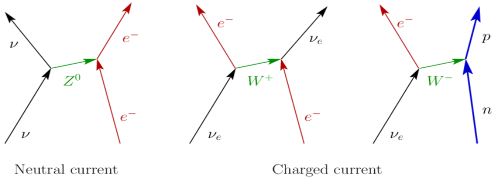

Neutrinos participate in EW interactions

Reactor neutrinos

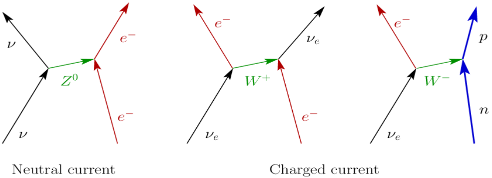

Neutrinos participate in EW interactions

- nuclear reactors are the major source of human-generated neutrinos (in *MeV* range) .

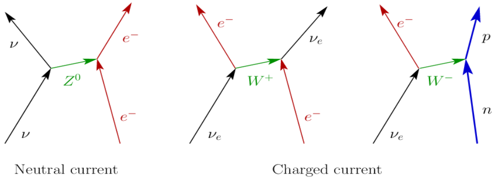

Neutrinos participate in EW interactions

- nuclear reactors are the major source of human-generated neutrinos (in MeV range) .
- the resultant neutron-rich daughter rapidly undergo additional beta decays

$$n \rightarrow p\bar{\nu}_e(\beta^- decay)$$
$$p \rightarrow n\nu_e(\beta^+ decay)$$
$$p + e^- \rightarrow n + \nu_e(electron\, capture)$$

Thermonuclear fusion reactions in the solar core produce energy and neutrinos

$$p + p \rightarrow d + e^{+} + \nu_e (E_\nu < 0.42 MeV)$$

$$^{7}Be + e^{-} \rightarrow ^{7}Li + \nu_e (E_\nu < 0.86 MeV)$$

$$^{8}B \rightarrow ^{8}Be + e^{+} \nu_e (E_\nu < 15 MeV)$$

$$^{3}He + p \rightarrow ^{4}He + e^{+} + \nu_e (E_\nu < 18.8 MeV)$$

Thermonuclear fusion reactions in the solar core produce energy and neutrinos

$p + p \rightarrow d + e^{+} + \nu_e (E_\nu < 0.42 MeV)$

${}^{7}Be + e^{-} \rightarrow {}^{7}Li + \nu_e (E_\nu < 0.86 MeV)$

${}^{8}B \rightarrow {}^{8}Be + e^{+} \nu_e (E_\nu < 15 MeV)$

${}^{3}He + p \rightarrow {}^{4}He + e^{+} + \nu_e (E_\nu < 18.8 MeV)$

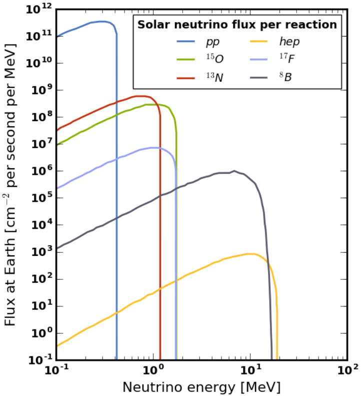

Thermonuclear fusion reactions in the solar core produce energy and neutrinos

$$p + p \rightarrow d + e^{+} + \nu_e (E_\nu < 0.42 MeV)$$
$$^{7}Be + e^{-} \rightarrow ^{7}Li + \nu_e (E_\nu < 0.86 MeV)$$
$$^{8}B \rightarrow ^{8}Be + e^{+} \nu_e (E_\nu < 15 MeV)$$
$$^{3}He + p \rightarrow ^{4}He + e^{+} + \nu_e (E_\nu < 18.8 MeV)$$

- pp chain is the dominant source in low energies and neutrinos are produced in $100 keV - 20 MeV$ range.

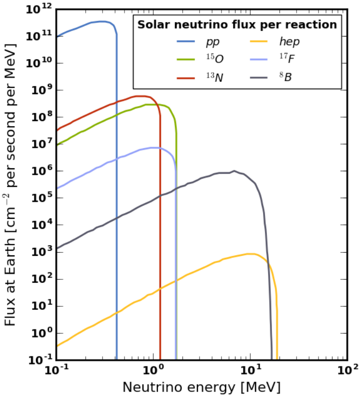

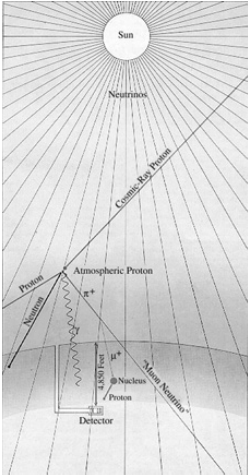

Neutrinos are also produced through cosmic nuclei-atmospheric neucli scattering (producing π/K)

$$\pi^{\pm}(K^{\pm}) \rightarrow \mu^{\pm} + \nu_{\mu}/\bar{\nu}_{\mu}$$

Atmospheric neutrinos

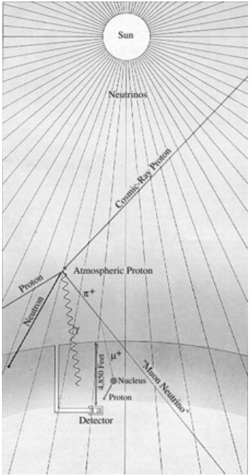

Neutrinos are also produced through cosmic nuclei-atmospheric neucli scattering (producing π/K)

$$\pi^{\pm}(K^{\pm}) \rightarrow \mu^{\pm} + \nu_{\mu}/\bar{\nu}_{\mu}$$

- Atmospheric neutrinos can be very energetic (GeV)

Other neutrino sources

- **Galactic and extra-galactic:** neutrinos can originate from the deleptonisation phase where protons and electrons are merged (Supernova)
- **Accelerator-based neutrinos:** neutrinos can be obtained from earthbound or cosmic accelerators in beam-dump experiments, where they are created in weak decays of short-lived hadrons.
- **Big Bang:** the universe's neutrinos background. they are notoriously difficult to detect, and the *CNB* might never be observed directly. There is, however, compelling indirect evidence for its existence.

Neutrino-nucleon scattering

The cross section for neutrino-nucleon scattering of $10GeV$ neutrinos is on the order of $7 \times 10^{-38} cm^2/nucleon$.

- Thus, for a target of $10m$ of solid iron the interaction probability

$$R = \sigma[N_A mol^{-1}/g \times]d\rho \approx 3 \times 10^{-10}$$

Neutrino-nucleon scattering

The cross section for neutrino-nucleon scattering of $10GeV$ neutrinos is on the order of $7 \times 10^{-38} cm^2/nucleon$.

- Thus, for a target of $10m$ of solid iron the interaction probability

$$R = \sigma[N_A mol^{-1}/g\times]d\rho \approx 3 \times 10^{-10}$$

- Neutrino–nucleon scattering of solar neutrinos of $(100keV)$ in the same material is $\approx 4 \times 10^{-12}$

Neutrino-nucleon scattering

The cross section for neutrino-nucleon scattering of $10GeV$ neutrinos is on the order of $7 \times 10^{-38} cm^2/nucleon$.

- Thus, for a target of $10m$ of solid iron the interaction probability

$$R = \sigma[N_A mol^{-1}/g \times] d\rho \approx 3 \times 10^{-10}$$

- Neutrino–nucleon scattering of solar neutrinos of ($100keV$) in the same material is $\approx 4 \times 10^{-12}$
- Energies in the several $100keV$ range are below the threshold($1.8MeV$) for inverse β decay $(\bar{\nu}_e + p \rightarrow n + e^)$

The cross section for neutrino-nucleon scattering of $10GeV$ neutrinos is on the order of $7 \times 10^{-38} cm^2/nucleon$.

- Thus, for a target of $10m$ of solid iron the interaction probability

$$R = \sigma[N_A mol^{-1}/g\times]d\rho \approx 3 \times 10^{-10}$$

- Neutrino–nucleon scattering of solar neutrinos of $(100keV)$ in the same material is $\approx 4 \times 10^{-12}$
- Energies in the several $100keV$ range are below the threshold$(1.8MeV)$ for inverse β decay $(\bar{\nu}_e + p \rightarrow n + e^)$
- **To get measurable interaction rates therefore high neutrino flux, a huge target and not too low energies are necessary.**

The world's first neutrino

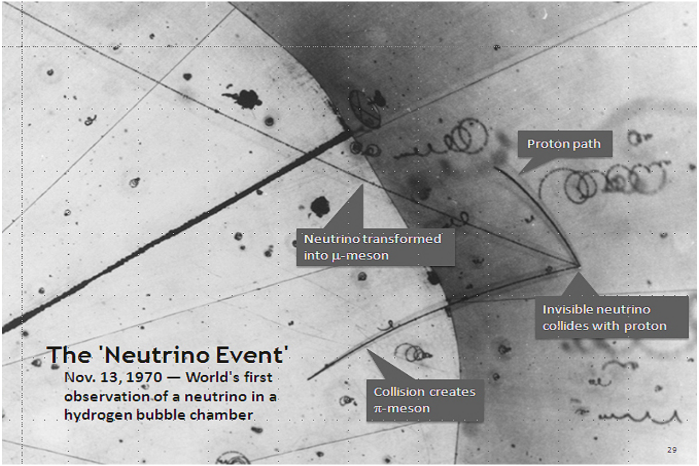

World's first neutrino detected in a hydrogen bubble chamber (at Argonne National Laboratory)

- **Scintillators:**

  place a scintillation detector next to a target (solution of cadmium chloride in water) Antineutrinos with an energy above the threshold of $1.8 MeV$ undergo IBD in the water. $\bar{\nu} + p \to e^+ n; e^- e^+ \to \gamma\gamma$.

  The neutrons captured by cadmium nuclei resulting in delayed gamma rays that are detected a few microseconds after the photons from a positron annihilation event.

- **Radiochemical methods:**
  based on the method suggested by Bruno Pontecorvo, consist of a tank filled with a chlorine containing fluid such as tetrachloroethylene.
  A neutrino converts a chlorine-37 atom into one of argon-37 via the charged current interaction.

- **Cherenkov(RICH) detectors:**
  detect Cherenkov light of muon or electron.
  In a Cherenkov detector, a large volume of clear material such as water or ice is surrounded by light-sensitive photomultiplier tubes.

- **Tracking calorimeters:**
  use alternating planes of absorber material and detector material. The absorber planes provide the energy while the detector planes provide the tracking information.
  Steel is a popular absorber choice, being relatively dense and inexpensive and having the advantage that it can be magnetised.
  Tracking calorimeters are only useful for high-energy (GeV range) neutrinos.
  At these energies, neutral current interactions appear as a shower of hadronic debris and charged current interactions are identified by the presence of the charged lepton's track (possibly alongside some form of hadronic debris.)

Homestake experiment

- The Homestake experiment (1965 – 1967, radiochemical) led by Raymond Davis, Jr. looked for solar neutrinos above $0.814MeV$ through IBD

$$\nu_e +^{37} Cl \rightarrow^{37} Ar + e^-$$

Homestake experiment

- The Homestake experiment ($1965 - 1967$, radiochemical) led by Raymond Davis, Jr. looked for solar neutrinos above $0.814 MeV$ through IBD

$$\nu_e +^{37} Cl \rightarrow^{37} Ar + e^-$$

- **The Homestake detector observed less than $1/3 SNU$ (One solar neutrino unit = one interaction per 10^{36} target atoms s^{-1}.) than it expected**

GALLEX experiment

The radiochemical GALLium EXperiments (GALLEX) looked for the solar pp neutrinos $(1991-1995)$.

- GALLEX monitored solar neutrinos above $233KeV$ through

$$^{71}Ga + v_e \rightarrow e^- +^{71} Ge$$

The radiochemical GALLium EXperiments (GALLEX) looked for the solar pp neutrinos $(1991-1995)$.

- GALLEX monitored solar neutrinos above $233KeV$ through

$$^{71}Ga + v_e \rightarrow e^- +^{71} Ge$$

- ^{71}Ge $(\tau_{1/2} = 11.43days)$ **(through electron-capture) emits Auger electrons and X-rays**

GALLEX experiment

The radiochemical GALLium EXperiments (GALLEX) looked for the solar pp neutrinos (1991 – 1995).

- GALLEX monitored solar neutrinos above $233KeV$ through

$$^{71}Ga + v_e \rightarrow e^- +^{71} Ge$$

- **^{71}Ge ($\tau_{1/2} = 11.43 days$) (through electron-capture) emits Auger electrons and X-rays**
- scatter solar neutrinos from the ^{71}Ga target while holding the BKG as low as possible.
- extract ^{71}Ge and transform them into a proportional chamber and count them.

GALLEX: detector

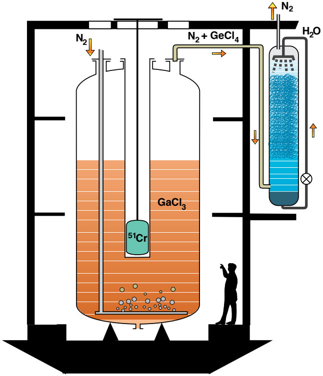

- 30.3 tons of $GaCl_3$ ($8.2M/lGaCl_3$ and $1.9M/l$ of HCl) in a cylinder($h = 8m; r = 1.9m$)
- gemrmanium is extracted by a large flow ($300m^3/h$) of N_2

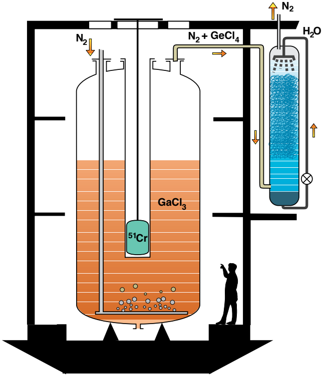

- 30.3 tons of $GaCl_3$ ($8.2M/lGaCl_3$ and $1.9M/l$ of HCl) in a cylinder($h = 8m; r = 1.9m$)
- gemrmanium is extracted by a large flow ($300m^3/h$) of N_2
- A typical solar exposure lasts about one month (followed by a 6-month period of counting ^{71}Ge)

GALLEX: detector

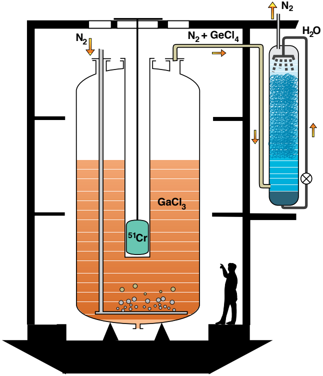

- 30.3 tons of $GaCl_3$ ($8.2M/lGaCl_3$ and $1.9M/l$ of HCl) in a cylinder($h = 8m; r = 1.9m$)
- gemrmanium is extracted by a large flow ($300m^3/h$) of N_2
- A typical solar exposure lasts about one month (followed by a 6-month period of counting ^{71}Ge)
- **^{51}Cr has been chosen as a convenient source of ν (through e-capture of ^{50}Cr) with the flux of $\approx 6 \times 10^{16} \nu/s$ in order validate the whole experiment.**

The GALLEX

Experiment	Results	Experiment/Predictions	
		BP [2]	TCL [3]
chlorine [15]	2.54 ± 0.20 SNU	0.27 ± 0.05	0.40 ± 0.10
Kamiokande [16]	2.80 ± 0.38 10^6 cm^{-2} s^{-1}	0.42 ± 0.09	0.64 ± 0.18
GALLEX [12]	70 ± 8 SNU	0.51 ± 0.06	0.57 ± 0.07
SAGE [13]	72 ± 13 SNU	0.53 ± 0.10	0.59 ± 0.11

Results of the solar neutrino experiments and comparison to the predictions from Bahcall and Pinson (BP) and Turck-Chieze and Loops (TCL).

The GALLEX

Experiment	Results	Experiment/Predictions	
		BP [2]	TCL [3]
chlorine [15]	2.54 ± 0.20 SNU	0.27 ± 0.05	0.40 ± 0.10
Kamiokande [16]	2.80 ± 0.38 10^6 cm^{-2} s^{-1}	0.42 ± 0.09	0.64 ± 0.18
GALLEX [12]	70 ± 8 SNU	0.51 ± 0.06	0.57 ± 0.07
SAGE [13]	72 ± 13 SNU	0.53 ± 0.10	0.59 ± 0.11

Results of the solar neutrino experiments and comparison to the predictions from Bahcall and Pinson (BP) and Turck-Chieze and Loops (TCL).

- Chlorine is mainly sensitive to the $\nu_{Be} and \nu_B$, Kamiokande to ν_B and GALLEX is sensitive to ν_{pp}

The GALLEX

Experiment	Results	Experiment/Predictions	
		BP [2]	TCL [3]
chlorine [15]	2.54 ± 0.20 SNU	0.27 ± 0.05	0.40 ± 0.10
Kamiokande [16]	2.80 ± 0.38 10^6 cm^{-2} s^{-1}	0.42 ± 0.09	0.64 ± 0.18
GALLEX [12]	70 ± 8 SNU	0.51 ± 0.06	0.57 ± 0.07
SAGE [13]	72 ± 13 SNU	0.53 ± 0.10	0.59 ± 0.11

Results of the solar neutrino experiments and comparison to the predictions from Bahcall and Pinson (BP) and Turck-Chieze and Loops (TCL).

- Chlorine is mainly sensitive to the $\nu_{Be} and \nu_B$, Kamiokande to ν_B and GALLEX is sensitive to ν_{pp}
- **deficit in all experiments shows something fundamental is missing** $\rightarrow$ *neutrino oscillation turned out to be the reason.*

Calorimetric neutrino detectors for high-energy neutrinos are based on the measurement of the total energy of the final-state hadrons produced in a neutrino–nucleon interaction.

Calorimetric neutrino detectors

Calorimetric neutrino detectors for high-energy neutrinos are based on the measurement of the total energy of the final-state hadrons produced in a neutrino–nucleon interaction.

- These calorimeters are mostly sandwiches consisting of alternating passive targets and active detectors

Calorimetric neutrino detectors

Calorimetric neutrino detectors for high-energy neutrinos are based on the measurement of the total energy of the final-state hadrons produced in a neutrino–nucleon interaction.

- These calorimeters are mostly sandwiches consisting of alternating passive targets and active detectors
- The large neutrino detectors at CERN (CDHS and Charm) were sampling detectors while KARMEN and SuperKamiokande are large-volume total-absorption devices

Calorimetric neutrino detectors

Calorimetric neutrino detectors for high-energy neutrinos are based on the measurement of the total energy of the final-state hadrons produced in a neutrino–nucleon interaction.

- These calorimeters are mostly sandwiches consisting of alternating passive targets and active detectors
- The large neutrino detectors at CERN (CDHS and Charm) were sampling detectors while KARMEN and SuperKamiokande are large-volume total-absorption devices
- Depending on which neutrino flavour is being detected the calorimeter must be sensitive not only to hadrons but also to electrons or muons.

NOMAD experiment

A precise knowledge of the cross section of (anti)neutrino-nucleus quasi-elastic scattering process (QEL) is important for the planning and analysis of any experiment which detects astrophysical, atmospheric or accelerator neutrinos.

NOMAD experiment

A precise knowledge of the cross section of (anti)neutrino-nucleus quasi-elastic scattering process (QEL) is important for the planning and analysis of any experiment which detects astrophysical, atmospheric or accelerator neutrinos.

- Neutrino Oscillation MAgnetic Detector (NOMAD) investigated the QEL process

$$\nu_\mu + n \to \mu^- + p$$
$$\bar{\nu}_{mu} + p \to \mu^+ + n$$

NOMAD experiment

A precise knowledge of the cross section of (anti)neutrino-nucleus quasi-elastic scattering process (QEL) is important for the planning and analysis of any experiment which detects astrophysical, atmospheric or accelerator neutrinos.

- Neutrino Oscillation MAgnetic Detector (NOMAD) investigated the QEL process

$$\nu_\mu + n \rightarrow \mu^- + p$$
$$\bar{\nu}_{mu} + p \rightarrow \mu^+ + n$$

- The main goals of the NOMAD experiment:
  - probing necluon internal structure and neutrino oscillations

NOMAD experiment: neutrino beam

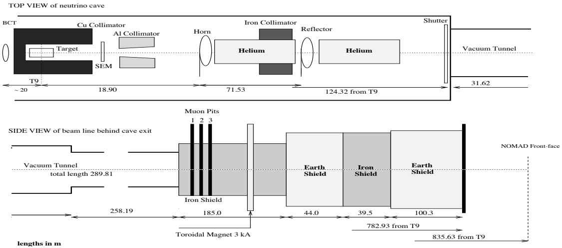

The general layout of the beam line

- $450GeV$ proton beam hit beryllium target $\rightarrow$ charged particles (mainly π^+ and K^+ mesons) produced around zero degrees subsequently decay producing neutrinos.

NOMAD experiment: neutrino beam

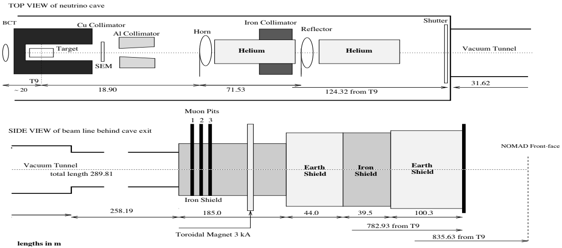

The general layout of the beam line

- mainly of ν_μ (with an about 7% admixture of $\bar{\nu}_\mu$ and less than 1% of $\nu_e / bar\nu_e$.

NOMAD experiment: detector

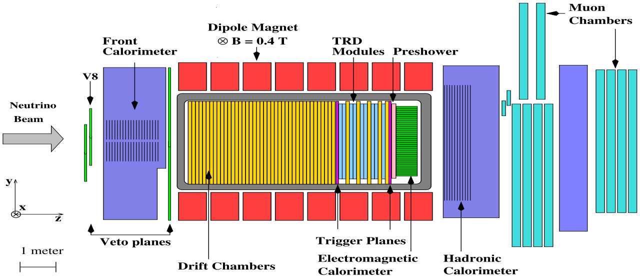

- The NOMAD detector consisted of an active target of 44 drift chambers with a total fiducial mass of $2.7 tons$, located in a 0.4 Tesla dipole magnetic field. The total volume of the drift chambers is about $3 \times 3 \times 4m^3$)

NOMAD experiment: detector

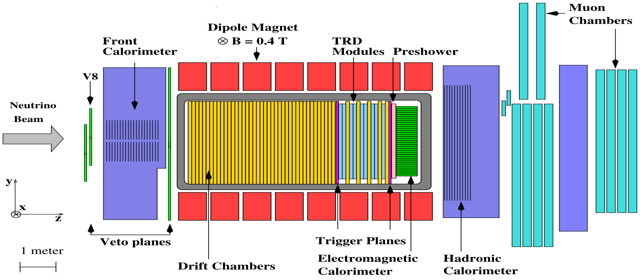

- Drift chambers, made of low Z material served the dual role of a nearly isoscalar target1 for neutrino interac- tions and of tracking medium.

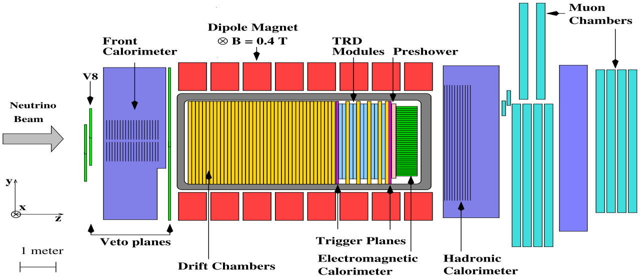

- Reconstructed tracks were used to determine the event topology (the assignment of tracks to vertices), to reconstruct the vertex position and the track parameters at each vertex and, finally, to identify the vertex type (primary, secondary, etc.).

NOMAD experiment: detector

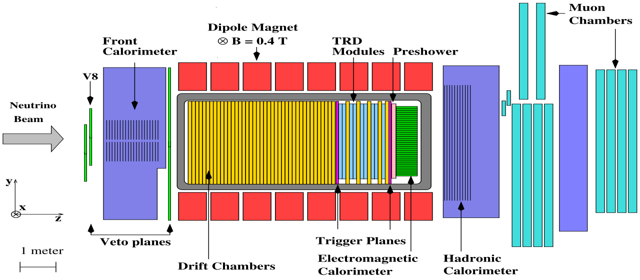

- A transition radiation detector (TRD) placed at the end of the active target was used for particle identification. Two scintillation counter trigger planes were used to trigger on neutrino interactions in the NOMAD active target.

NOMAD experiment: detector

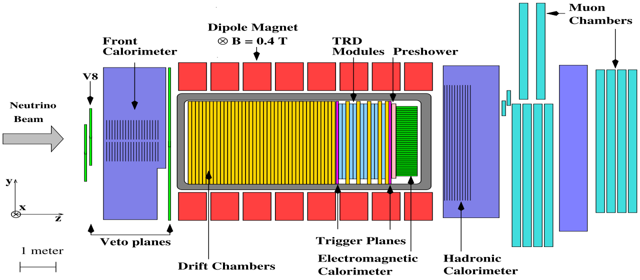

- A lead-glass electromagnetic calorimeter located downstream of the tracking region provided an energy resolution of $3.2/\sqrt{E} \oplus 1\%$ for electromagnetic showers and was crucial to measure the total energy flow in neutrino interactions.

NOMAD experiment: detector

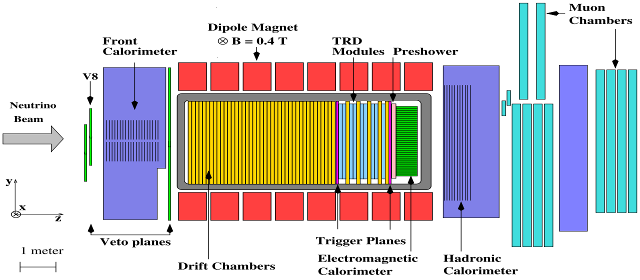

- In addition, an iron absorber and a set of muon chambers located after the electromagnetic calorimeter was used for muon identification, providing a muon detection efficiency of 97% for momenta greater than $5GeV/c$.

NOMAD experiment: results

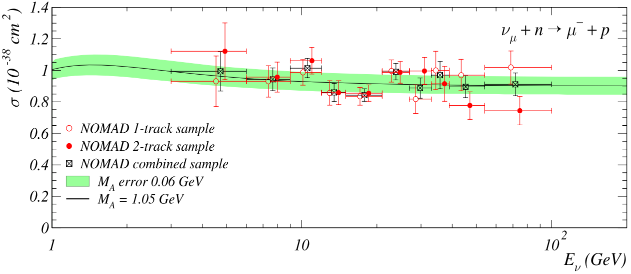

$\nu_\mu + n \to \mu^- + p$ quasi-elastic scattering cross-section

- the axial structure of the nucleon. Provide information on spin-isospin distributions (i.e. they can discriminate between 'upness' and 'downness') Provide insight into the differences between proton and neutron structure Isospin symmetry violation Strangeness contributions.

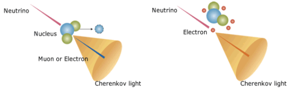

The generated charged particle emits the Cherenkov light.

- signals:

$$\nu_l + e^- \rightarrow \nu_l + e^- (ES)$$
$$\nu_l + p \rightarrow l^- + n(CC)$$

- **Physics aims**:
  - neutrino oscillation
  - neutrinos mass
  - neutrino flavors

Super-Kamiokande experiment: detector

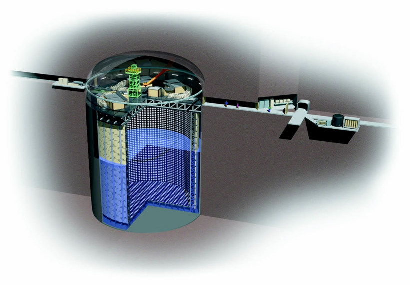

- **Water tank:**
  The Super-Kamiokande detector consists of a cylindrical stainless steel tank, $39.3m$ in diameter and $41.4m$ in height filled with $50ktons$ of pure water.

Super-Kamiokande experiment: detector

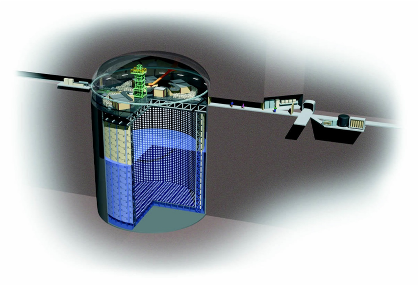

- **ID:**
  11129 ($20 - inch$) inward-facing PMTs are evenly placed on the wall of the ID
  in order to protect the detector against PMT implosions as happened in 2001, each ID PMT is enclosed in a FRP housing with an acrylic window covering the photocathode area so that the shock wave does not occur even if one of the PMTs imploded.

Super-Kamiokande experiment: detector

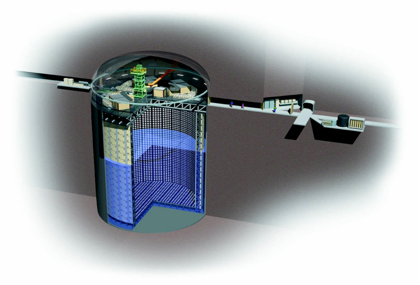

- **OD:**
  1,885 (8-inch) evenly-spaced PMTs facing outward.
  Unlike the ID, the spaces between the PMTs are covered with a reflective material Tyvek which has about 90% reflectivity at 400 nm in order to increase the photon collection efficiency in the OD.

Super-Kamiokande experiment: detector

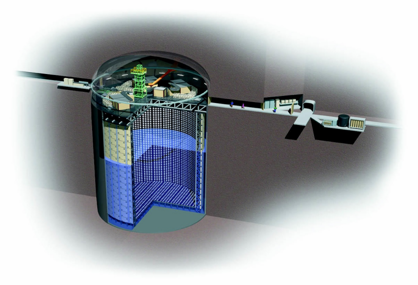

- each PMT is surrounded by square wavelength-shifting plates to transfer Cherenkov UV to visible light

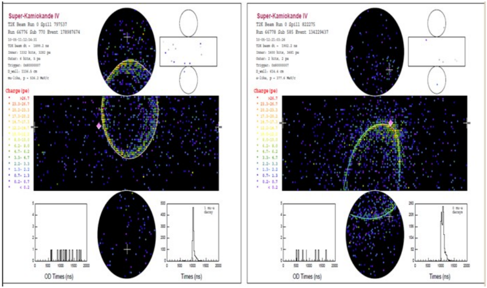

- electron(left) and muon(right) events in the atmospheric neutrino data. The ring for muon is sharper than electron
- Each dot represents a PMT which detected Cherenkov photons, and the colour scale represents the number of photons detected at each PMT.

Super-Kamiokande experiment: results

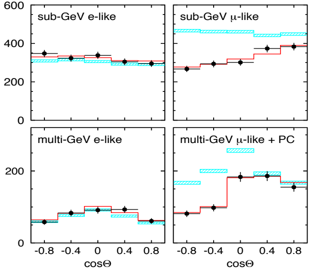

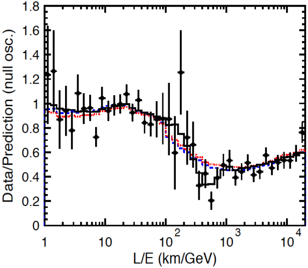

- left:Zenith angle distributions of e-like and μ-like events in SK with momenta above GeV (top) and below GeV (bottom). The boxes show expectation assuming no oscillations.
  right: ratio of data from SK to Monte Carlo expectation assuming no oscillation, as a function of reconstructed L/E. The black histogram is a fit to a two flavour oscillation hypothesis.

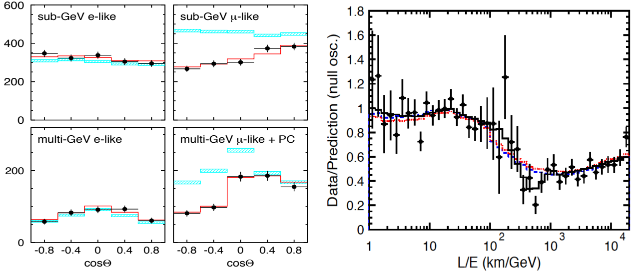

- whereas the flux of electron-neutrinos has almost no zenith angle dependence, the flux of down-going ($\cos\theta = 1$) muon-neutrinos significantly exceeds the flux of up-going ν_μ. **This can be simply interpreted in terms of neutrino oscillations**

SNO experiment

- **The $2km$ underground Sudbury Neutrino Observatory (SNO, 1999-current) has been looking for neutrinos through:**

$$\nu_l + e^- \to \nu_l + e^- (ES)$$
$$\nu_e + d \to e^- + p + p (CC)$$
$$\nu_l + d \to \nu_l + n + p (NC)$$

SNO experiment

- **The $2km$ underground Sudbury Neutrino Observatory (SNO, 1999-current) has been looking for neutrinos through:**

$$\nu_l + e^- \to \nu_l + e^- (ES)$$
$$\nu_e + d \to e^- + p + p(CC)$$
$$\nu_l + d \to \nu_l + n + p(NC)$$

- **Physics aims:**
  - **solve the solar neutrino problem**
  - neutrino oscillations
  - information on muon neutrinos and tau neutrinos

SNO experiment

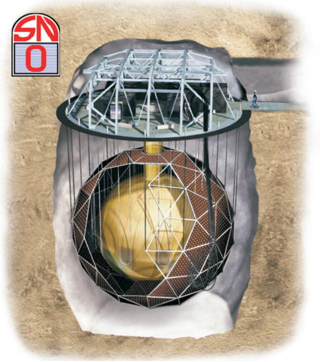

- 1000 tonnes of ultrapure heavy water (99.917% ^2H) contained within a 12m diameter, 5.6cm thick transparent acrylic vessel.

  Highly enriched heavy water was required because $\frac{\sigma^{^1H}_{n-capture}}{\sigma^{^2H}_{n-capture}} = 640 \rightarrow 99.85\%$ enrichment

SNO experiment

- 1000 tonnes of ultrapure heavy water (99.917% ^2H) contained within a $12m$ diameter, $5.6cm$ thick transparent acrylic vessel.

  Highly enriched heavy water was required because $\frac{\sigma^{^1H}_{n-capture}}{\sigma^{^2H}_{n-capture}} = 640 \rightarrow 99.85\%$ enrichment

- 9438 PMTs eyes on an $18-m$ diameter support structure.

SNO experiment

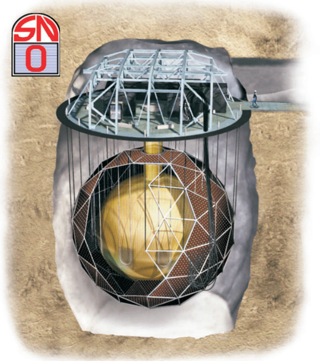

- 1000 tonnes of ultrapure heavy water (99.917% ^2H) contained within a 12m diameter, 5.6cm thick transparent acrylic vessel.

  Highly enriched heavy water was required because $\frac{\sigma^{1H}_{n-capture}}{\sigma^{2H}_{n-capture}} = 640 \rightarrow 99.85\%$ enrichment

- 9438 PMTs eyes on an $18 - m$ diameter support structure.
- The entire cavity outside the acrylic vessel was filled with ultrapure light water.

SNO: water system

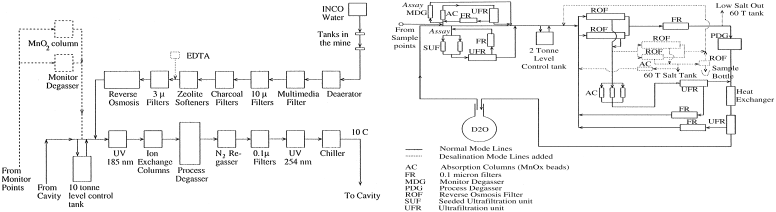

left: H_2O right: D_2O

- two water systems at SNO: one for the ultrapure light water (H_2O) and one for the heavy water (D_2O).

SNO: water system

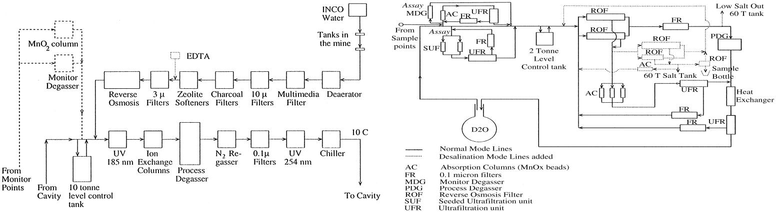

left: H_2O right: D_2O

- After running H_2O through a series of filtration systems, a degassser is used to reduce the levels of oxygen and radon, then the water is cooled to $10C$ before it goes into the cavity.
  , The H_2O is continuously circulated to remove ions, organic materials, and suspended solids.

SNO: water system

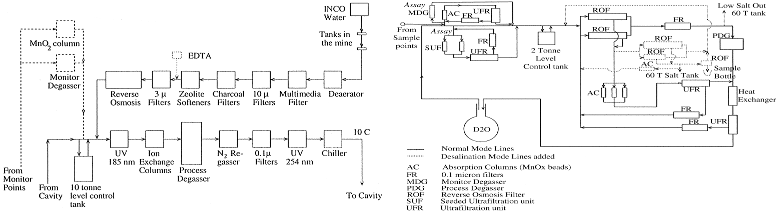

left: H_2O right: D_2O

- The heavy water is first passed through ion-exchange columns to reduce its ionic content, before it goes into the acrylic vessel.
  After the SNO detector is filled, the D_2O is recirculated to maintain its purity and assay it to make an accu- rate background determination.

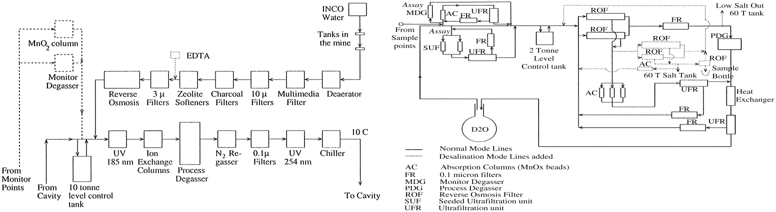

left: H_2O right: D_2O

- The D_2O and H_2O have to be isolated from the laboratory air to prevent radon from getting in, (A cover gas like N_2.)

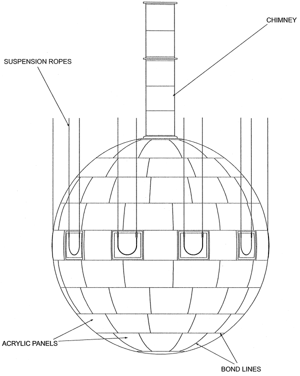

The primary design criteria for the containment vessel are:

- isolate $1000t$ of D_2O from surrounding H_2O
- minimize the radioactive impurities.
- maximize optical performance
- a total of 122 ultraviolet transmitting (UVT) acrylic panels were used in the construction of the spherical part of the containment vessel. (uncompromising integrity as well as excellent transparency and very low radioactivity, ultraviolet-transmitting)

SNO: photomultiplier tubes

- 9438 inward-facing PMTs, which provide a photocathode coverage of 31%. To improve the light-collection efficiency, a $27 - cm$ entrance-diameter light concentrator is mounted on each PMT, increasing the effective photocathode coverage to $\approx 54\%$.

SNO: photomultiplier tubes

- 9438 inward-facing PMTs, which provide a photocathode coverage of 31%. To improve the light-collection efficiency, a $27 - cm$ entrance-diameter light concentrator is mounted on each PMT, increasing the effective photocathode coverage to $\approx 54\%$.
- **another 91 PMTs without concentrators were mounted facing outward to detect light from muons and other sources in the region exterior to the PM supporting structure.**

SNO: run I

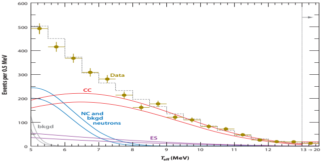

$$\phi_{\text{CC}} = 1.76^{+0.06}_{-0.05}\,(\text{stat.})^{+0.09}_{-0.09}\,(\text{syst.}),$$

$$\phi_{\text{ES}} = 2.39^{+0.24}_{-0.23}\,(\text{stat.})^{+0.12}_{-0.12}\,(\text{syst.}),$$

$$\phi_{\text{NC}} = 5.09^{+0.44}_{-0.43}\,(\text{stat.})^{+0.46}_{-0.43}\,(\text{syst.}).$$

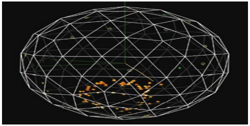

$$\phi_{\nu_e} = 1.76^{+0.05}_{-0.05}\,(\text{stat.})^{+0.09}_{-0.09}\,(\text{syst.})$$

$$\phi_{\nu_{\mu\tau}} = 3.41^{+0.45}_{-0.45}\,(\text{stat.})^{+0.48}_{-0.45}\,(\text{syst.}),$$

- The first operation (1999 – 2001) using pure heavy water as the central detection medium.

SNO: run I

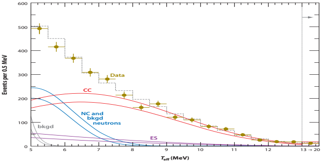

$$\phi_{\rm CC} = 1.76^{+0.06}_{-0.05}\,(\text{stat.})^{+0.09}_{-0.09}\,(\text{syst.}),$$

$$\phi_{\rm ES} = 2.39^{+0.24}_{-0.23}\,(\text{stat.})^{+0.12}_{-0.12}\,(\text{syst.}),$$

$$\phi_{\rm NC} = 5.09^{+0.44}_{-0.43}\,(\text{stat.})^{+0.46}_{-0.43}\,(\text{syst.}).$$

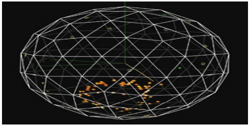

$$\phi_{\nu_e} = 1.76^{+0.05}_{-0.05}\,(\text{stat.})^{+0.09}_{-0.09}\,(\text{syst.})$$

$$\phi_{\nu_{\mu\tau}} = 3.41^{+0.45}_{-0.45}\,(\text{stat.})^{+0.48}_{-0.45}\,(\text{syst.}),$$

- neutron-capture on the deuterons in D_2O releases $6.25MeV$ gamma rays.
  - The gamma rays (Compton) scatter of the atomic electrons
  - the electrons above the Cherenkov threshold radiate Cherenkov light.

SNO: run I

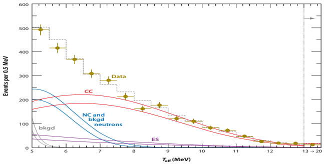

$$\phi_{CC} = 1.76^{+0.06}_{-0.05}\,(\text{stat.})^{+0.09}_{-0.09}\,(\text{syst.}),$$

$$\phi_{ES} = 2.39^{+0.24}_{-0.23}\,(\text{stat.})^{+0.12}_{-0.12}\,(\text{syst.}),$$

$$\phi_{NC} = 5.09^{+0.44}_{-0.43}\,(\text{stat.})^{+0.46}_{-0.43}\,(\text{syst.}).$$

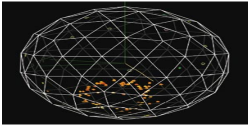

$$\phi_{\nu_e} = 1.76^{+0.05}_{-0.05}\,(\text{stat.})^{+0.09}_{-0.09}\,(\text{syst.})$$

$$\phi_{\nu_{\mu\tau}} = 3.41^{+0.45}_{-0.45}\,(\text{stat.})^{+0.48}_{-0.45}\,(\text{syst.}),$$

- with a $6.75MeV$ cut on the T_{eff}, NC reaction was suppressed significantly.
  – The CC and ES reactions could be resolved through use of the strong directional dependence of the ES reaction.
  neutrino flux are in $10^6 cm^{-2}s^{-1}$

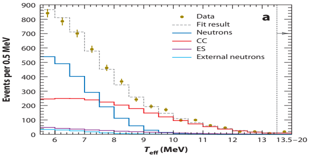

$$\phi_{CC} = 1.68^{+0.06}_{-0.06}\,(\text{stat.})^{+0.08}_{-0.09}\,(\text{syst.}),$$
$$\phi_{ES} = 2.35^{+0.22}_{-0.22}\,(\text{stat.})^{+0.15}_{-0.15}\,(\text{syst.}),$$
$$\phi_{NC} = 4.94^{+0.21}_{-0.21}\,(\text{stat.})^{+0.38}_{-0.34}\,(\text{syst.}),$$

- (2001-2003) salt added to D_2O
  1) the neutron-capture efficiency increases (by a factor of three)
  2) Cherenkov light also increases because more energy is released in the neutron capture on ^{35}Cl.
  3) neutron capture on ^{35}Cl typically produces multiple gamma rays $\rightarrow$ multiple electrons, whereas the CC and ES reactions produce single electrons.

SNO: run II

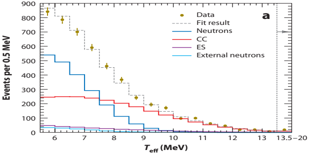

$$\phi_{CC} = 1.68^{+0.06}_{-0.06}\,(\text{stat.})^{+0.08}_{-0.09}\,(\text{syst.}),$$
$$\phi_{ES} = 2.35^{+0.22}_{-0.22}\,(\text{stat.})^{+0.15}_{-0.15}\,(\text{syst.}),$$
$$\phi_{NC} = 4.94^{+0.21}_{-0.21}\,(\text{stat.})^{+0.38}_{-0.34}\,(\text{syst.}),$$

- the isotropy of the Cherenkov light from neutron-capture events relative to CC and ES events allows good statistical separation 3-signals
  $\rightarrow$ precise measurement of the NC flux, independent of assumptions about the CC and ES energy spectra.

SNO : run III

$$\phi_{\text{CC}} = 1.67^{+0.05}_{-0.04}\,(\text{stat.})^{+0.07}_{-0.08}\,(\text{syst.}),$$
$$\phi_{\text{ES}} = 1.77^{+0.24}_{-0.21}\,(\text{stat.})^{+0.09}_{-0.10}\,(\text{syst.}),$$
$$\phi_{\text{NC}} = 5.54^{+0.33}_{-0.31}\,(\text{stat.})^{+0.36}_{-0.34}\,(\text{syst.}),$$

- The extraction of the three neutrino-interaction signals from SNO requires breakdown of the Cherenkov light signals into the three components on a statistical basis.

$$\phi_{\mathrm{CC}} = 1.67^{+0.05}_{-0.04}\,(\mathrm{stat.})^{+0.07}_{-0.08}\,(\mathrm{syst.}),$$
$$\phi_{\mathrm{ES}} = 1.77^{+0.24}_{-0.21}\,(\mathrm{stat.})^{+0.09}_{-0.10}\,(\mathrm{syst.}),$$
$$\phi_{\mathrm{NC}} = 5.54^{+0.33}_{-0.31}\,(\mathrm{stat.})^{+0.36}_{-0.34}\,(\mathrm{syst.}),$$

- it is possible to detect the NC directly through use of neutron-sensitive proportional counters.
  although neutrons do not typically cause ionization, the addition of a nuclide with high neutron cross-section allows the detector to respond to neutrons ^3He, ^6Li, ^{10}B.
  $^3He + n \rightarrow {}^1H^3H^+ + e^-$

SNO : run III

$$\phi_{\mathrm{CC}} = 1.67^{+0.05}_{-0.04}\,(\mathrm{stat.})^{+0.07}_{-0.08}\,(\mathrm{syst.}),$$
$$\phi_{\mathrm{ES}} = 1.77^{+0.24}_{-0.21}\,(\mathrm{stat.})^{+0.09}_{-0.10}\,(\mathrm{syst.}),$$
$$\phi_{\mathrm{NC}} = 5.54^{+0.33}_{-0.31}\,(\mathrm{stat.})^{+0.36}_{-0.34}\,(\mathrm{syst.}),$$

- after removing salt from D_2O, an array of (40) proportional counters attached to anchor points on the inner surface filled with an $85:15$ ^3He and CF_4 inserted in the heavy water to detect neutrons.

Additional material

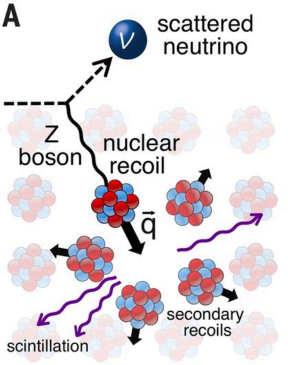

Coherent Elastic Neutrino-Nucleus Scattering (*CEνNS*):

- For a small momentum exchange $qR_N < 1$ a long-wavelength Z boson sees the whole nucleus.

Neutrino-nucleon scattering

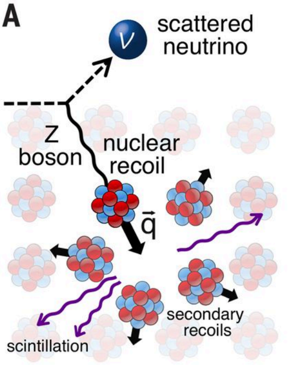

Coherent Elastic Neutrino-Nucleus Scattering ($CE\nu NS$)**:**

- For a small momentum exchange $qR_N < 1$ a long-wavelength Z boson sees the whole nucleus.
- An inconspicuous low-energy nuclear recoil is the only observable.

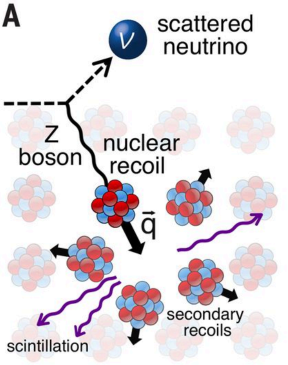

Coherent Elastic Neutrino-Nucleus Scattering ($CE\nu NS$)**:**

- For a small momentum exchange $qR_N < 1$ a long-wavelength Z boson sees the whole nucleus.
- An inconspicuous low-energy nuclear recoil is the only observable.
- However, the probability of neutrino interaction increases dramatically with the square of the number of neutrons in the target nucleus.

Neutrino-nucleon scattering

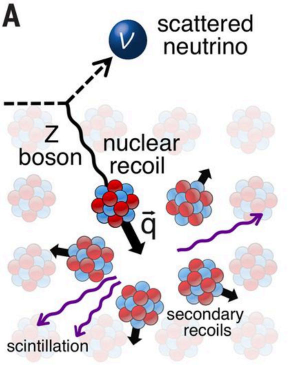

Coherent Elastic Neutrino-Nucleus Scattering ($CE\nu NS$):

- For a small momentum exchange $qR_N < 1$ a long-wavelength Z boson sees the whole nucleus.
- An inconspicuous low-energy nuclear recoil is the only observable.
- However, the probability of neutrino interaction increases dramatically with the square of the number of neutrons in the target nucleus.
- In scintillating materials, the ensuing dense cascade of secondary recoils dissipates a fraction of its energy as detectable light.

Neutrino-nucleon scattering

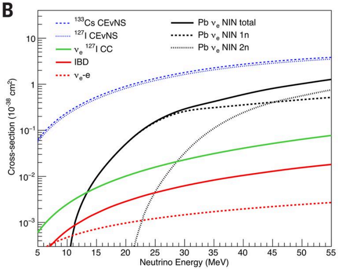

Total cross-sections from *CEνNS* and some known neutrino couplings.

- because of their similar nuclear masses, cesium and iodine respond to *CEνNS* almost identically.

Neutrino-nucleon scattering

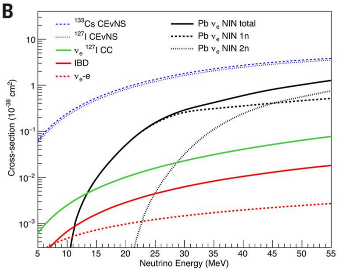

Total cross-sections from *CEνNS* and some known neutrino couplings.

- because of their similar nuclear masses, cesium and iodine respond to $CE\nu NS$ almost identically.
- the present $CE\nu NS$ measurement involves neutrino energies in the range $16 - 53 MeV$

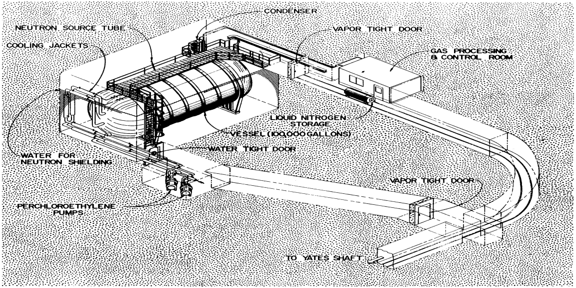

- The apparatus consists of a single horizontal steel tank with dished ends, $6.1m$ in diameter and $14.6m$ long, containing 615 metric tons of tetrachloroethylene, C_2Cl_4 .

Homestake experiment

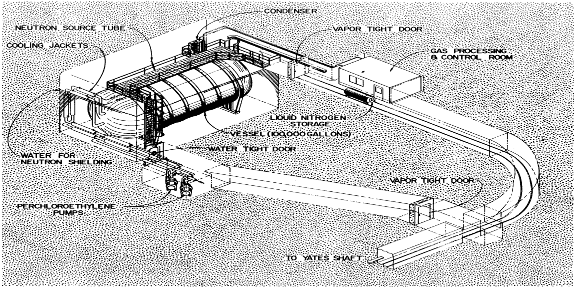

- **solar neutrinos convert a very small number of the ^{37}Cl atoms into $^{37}Ar \rightarrow$ the challenge is to remove these ^{37}Ar atoms efficiently from the detector and determine their number.**

Homestake experiment

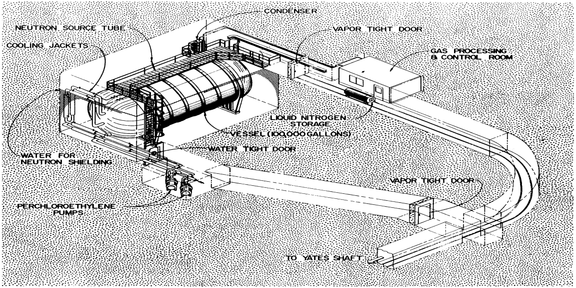

- The system for removing the argon from the tank involves two steps:
  1) maintaining an equilibrium between the Ar_{gas} and $Ar_{disolved}$ by bubbling helium through the tank
  2) sweeping the helium atmosphere of the tank through an external, cryogenically cooled absorber that traps the argon but allows the helium to pass through and return to the detector.

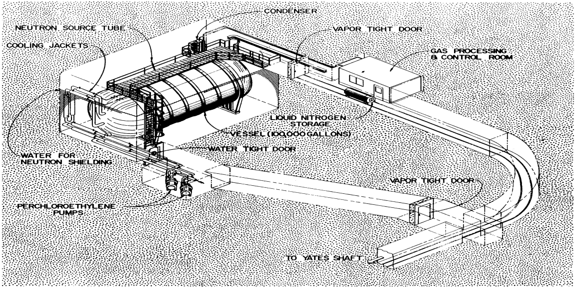

- **The Homestake detector observed less than $1/3SNU$ (One solar neutrino unit = one interaction per 10^{36} target atoms s^{-1}.) than it expected**

The CDHS

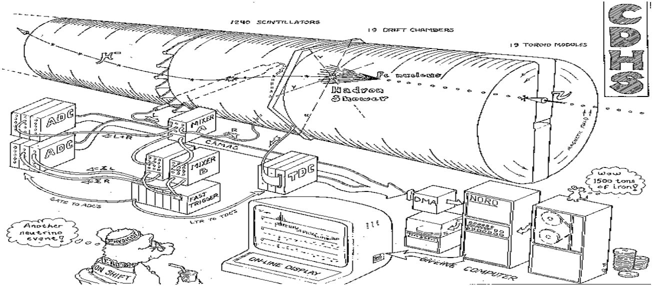

- **probing deep inelastic neutrino interactions in iron.**

$$\nu_\mu + Fe \rightarrow \nu_\mu + X(NC)$$
$$\nu_\mu + Fe \rightarrow \mu + X(CC)$$

The CDHS

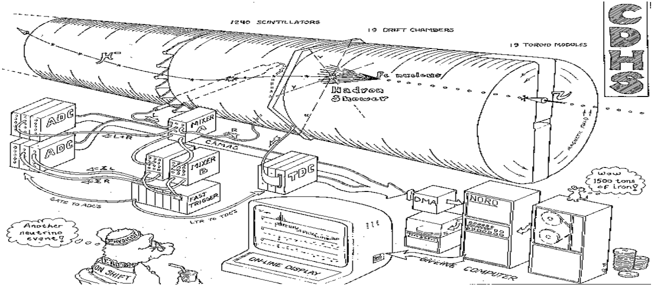

.

- The detector is a magnetized iron cylinder (3.85m in diameter and mass of 1250$tons$) and combined the functions of a muon spectrometer and hadron calorimeter. It consisted of 19 magnetized iron modules (0.75m), separated from each other by scintillators and wire drift chambers.

The CDHS

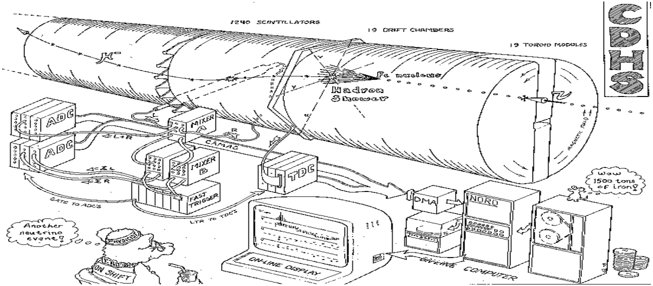

.

- drift chambers are inserted between the modules for muon tracking. The scintillator structure allows one to measure the position of the shower

The CDHS

- The detector records neutrino-iron interactions producing hadronic showers of energies above the trigger threshold of about $3GeV$.

The CDHS

- The detector records neutrino-iron interactions producing hadronic showers of energies above the trigger threshold of about $3GeV$.
- If the active elements in a total-absorption or sampling calorimetric system provide some spatial information, one is able to distinguish different final-state products in such neutrino tracking detectors.

The CDHS

- The detector records neutrino-iron interactions producing hadronic showers of energies above the trigger threshold of about $3GeV$.
- If the active elements in a total-absorption or sampling calorimetric system provide some spatial information, one is able to distinguish different final-state products in such neutrino tracking detectors.
- **a di-muon event in the CDHS detector.**

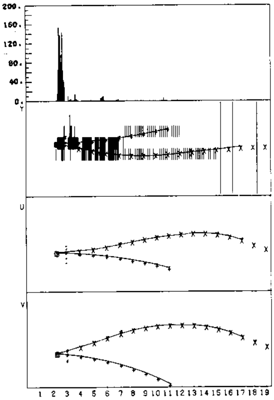

(b)

The Karlsruhe Rutherford Medium Energy Neutrino(KARMEN) performed at the neutron spallation facility ISIS of the Rutherford Appleton Laboratory looking for:

KARMEN experiment

The Karlsruhe Rutherford Medium Energy Neutrino(KARMEN) performed at the neutron spallation facility ISIS of the Rutherford Appleton Laboratory looking for:

$$p + Ta - D_2O \rightarrow \pi^+ + X$$

$$\pi^+ \rightarrow \mu^+ + \nu_\mu$$

$$\mu^+ \rightarrow e^+ + \nu_e + \bar{\nu}_\mu$$

KARMEN experiment

The Karlsruhe Rutherford Medium Energy Neutrino(KARMEN) performed at the neutron spallation facility ISIS of the Rutherford Appleton Laboratory looking for:

$$p + Ta - D_2O \to \pi^+ + X$$
$$\pi^+ \to \mu^+ + \nu_\mu$$
$$\mu^+ \to e^+ + \nu_e + \bar{\nu}_\mu$$

- **Major physics aims:**
  - the measurement of charged/neutral current (CC/NC)
  - neutrino-nucleon interactions
  - $\mu - e$ universality and the search for neutrino oscillations

KARMEN: neutrino beam

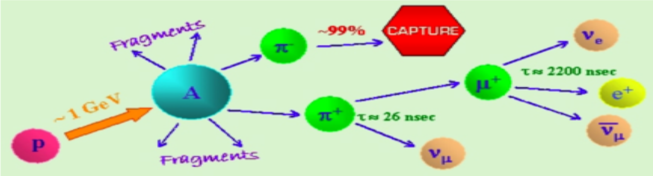

- **The neutron spallation facility ISIS produced (by stopping $800MeV$ protons in a beam dump $Ta - D_2O$ target) a ν-source with identical intensities for all neutrino flavors emitted**
- Spallation refers to nuclear reactions that occurs when energetic hadrons (for example, protons, neutrons, or pions) hits a neuclus target

KARMEN: neutrino beam

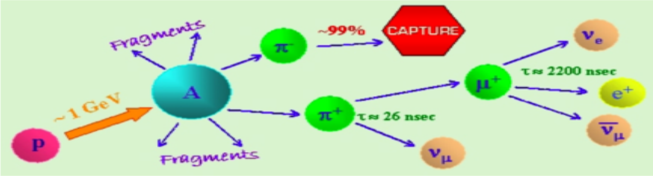

- **The neutron spallation facility ISIS produced (by stopping $800MeV$ protons in a beam dump $Ta - D_2O$ target) a ν-source with identical intensities for all neutrino flavors emitted**
- Spallation refers to nuclear reactions that occurs when energetic hadrons (for example, protons, neutrons, or pions) hits a neuclus target
- $\Phi_\nu = 6.37 \times 10^{13} \nu/s$ per flavor for p-beam current $I_p = 200\mu A$

KARMEN: detector

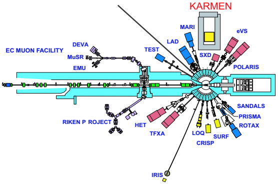

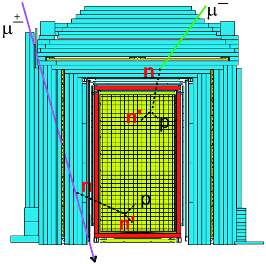

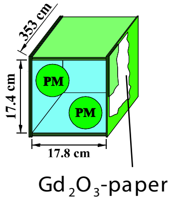

- **The KARMEN-detector was constructed as a large volume liquid scintillation calorimeter.**

KARMEN: detector

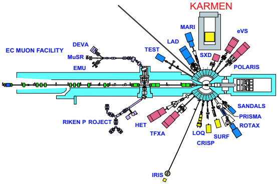

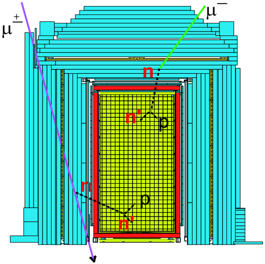

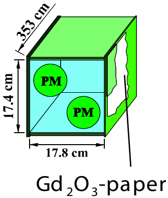

- The central part of the detector consists of a $6 \times 3.53 \times 3.20 m^3$ stainless steel tank($m = 7000t$) filled with $65000l$ of a dedicated liquid scintillator. The liquid scintillator is made of 75% vol. parrafin, 25% vol. pseudocumene

KARMEN: detector

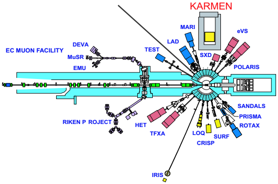

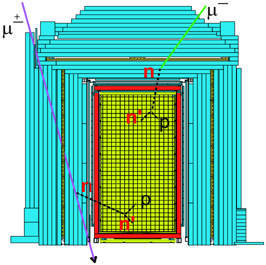

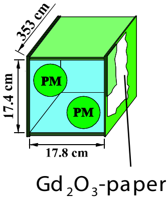

- The central scintillation calorimeter and the inner veto counters are segmented by double acrylic walls with an air gap allowing efficient light transport via total internal reflection of the scintillation light at the module walls.

KARMEN: detector

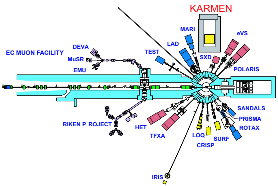

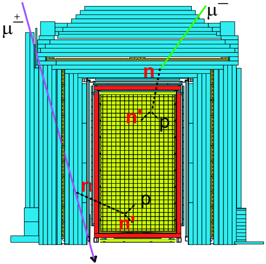

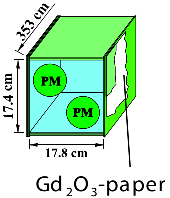

- **The event position is determined by the individual module and the time difference of the PM signals at each end of this module.**

KARMEN: $\bar{\nu}_\mu \leftrightarrow \bar{\nu}_e$ search results

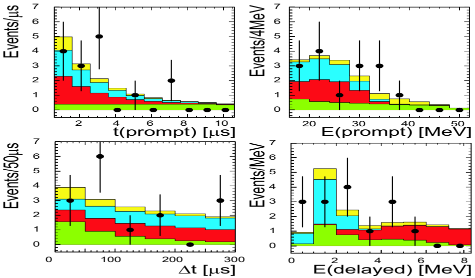

KARMEN 15 coincidence candidates after final cuts

- $\sum_{bkg} = 15.8 \pm 0.5 events$
- **extracted number of sequences is in excellent agreement with the background expectation, consistent with no additional $\bar{\nu}_e$ signal**

DONUT experiment

The tau neutrino, nu_{τ}, was added to the Standard Model after τ lepton discovery in 1975.

DONUT experiment

The tau neutrino, nu_τ, was added to the Standard Model after τ lepton discovery in 1975.

- The difficulty of measuring ν_τ interactions was due to the relative scarcity of the sources of ν_τ and the lack of sufficiently powerful detection methods to unambiguously identify the short-lived τ lepton.

The tau neutrino, nu_τ, was added to the Standard Model after τ lepton discovery in 1975.

- The difficulty of measuring ν_τ interactions was due to the relative scarcity of the sources of ν_τ and the lack of sufficiently powerful detection methods to unambiguously identify the short-lived τ lepton.
- Direct Observation of Nu-Tau (DONuT) experiment was designed to overcome these challenges

$$\nu_\tau + N \to \tau + X(SIG)$$
$$\nu_{e,\mu} + N \to e/\mu + [D/D_s/\Lambda] + X(BKG1)$$
$$\nu_l + N \to \nu_l + h^\pm; h^\pm + X \to \tau_{fake} + X^0(BKG2)$$

DONUT experiment: neutrino beam

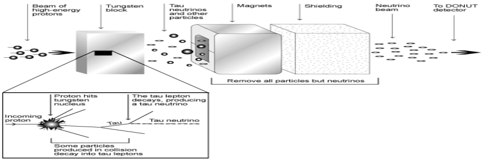

- The $800GeV$ protons from the Tevatron were stopped in a beamdump in the form of a solid block of tungsten alloy. The typical intensity was 8×10^{12} protons for 20 seconds each minute

DONUT experiment: neutrino beam

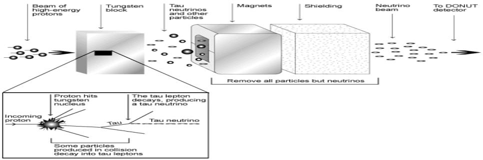

- Neutrinos in the DONuT beam originated from decays of particles within the hadron shower created by a primary proton interaction.

DONUT experiment: neutrino beam

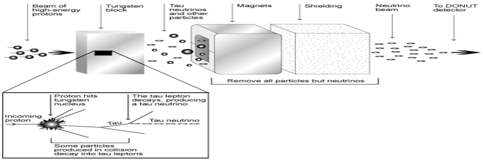

- **only 3% of the neutrino flux is ν_τ and most of them originated in leptonic decays of $D_s \to \tau\nu_{tau}$**

DONUT experiment: detector

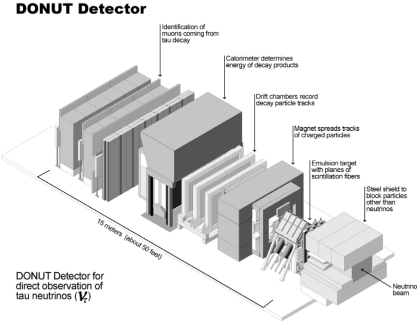

- **The Trigger Counters:**
  At least two high-momentum charged particle tracks coming from the emulsion targets and no incoming charged particles. Charged particles entering the upstream side were rejected by the veto wall.

DONUT experiment: detector

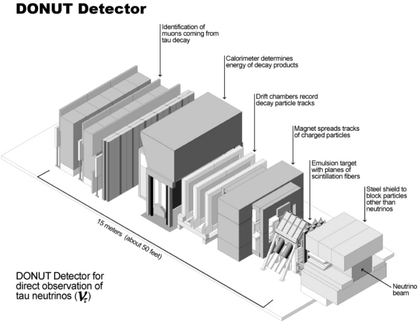

- **The Scintillating Fiber Tracking System:**
  The scintillating fiber planes provided position measurements for several sampling points along the track.

DONUT experiment: detector

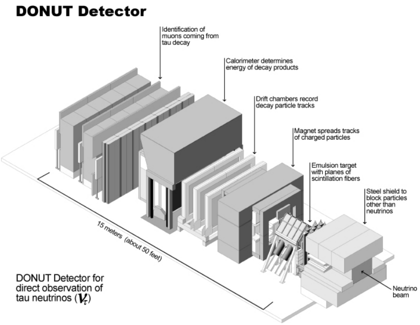

- **Downstream Tracking:**
  Charged particle tracks coming from the neutrino interaction vertex and identified in the scintillating fiber system give information about the neutrino interaction parameters. The particle momentum for these tracks was determined through the combination of drift chamber tracking and deflection in a

DONUT experiment: detector

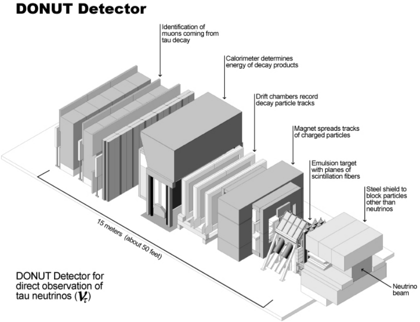

- **The Electromagnetic Calorimeter:**
  tau decays produce high-energy electrons. As they pass through material, these electrons generate electromagnetic showers that can be identified in the electromagnetic calorimeter (EMCAL), which provided an estimate for the electromagnetic energy of individual particles.

DONUT experiment: detector

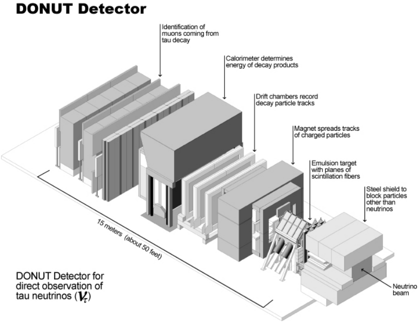

- **Muon Identification:**
  A muon neutrino charged-current interaction can be uniquely identified by the muon produced in the interaction.

DONUT experiment

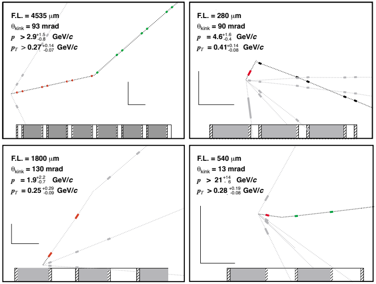

- The four ν_τ CC interaction events. The scale is given by the perpendicular lines with the vertical line representing $0.1mm$ and the horizontal $1mm$. The target material is shown by the bar at the bottom of each part of the figure representing steel (shaded), emulsion (cross hatched) and plastic (no shading)

DONUT experiment

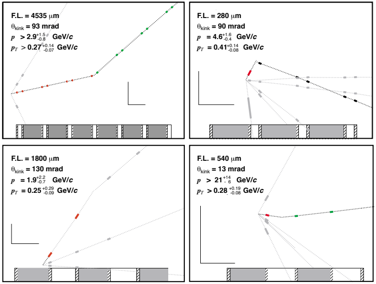

- out of 203 located neutrino interactions four events have a track that meets all the requirements for τ decays . The total background is estimated to b e $\sum_{bkg} = 0.34 \pm 0.05$ $\rightarrow > 4\sigma$ $\rightarrow$discovery